# Triboelectric characteristics and separation of magnesite and quartz

by Z. Zhang[1,3], Y. Xu[1,2], H. Wang[1,2], J. Shi[1,2], J. Niu[1,2], and Z. Zhang[1,2]

**Affiliation:**
[1]Key Laboratory of Coal Processing and Efficient Utilization of Ministry of Education, China University of Mining & Technology, Xuzhou, Jiangsu, China
[2]School of Chemical Engineering, China University of Mining and Technology, Xuzhou, Jiangsu, China
[3]Department of Chemical and Biomolecular Engineering, National University of Singapore, Singapore

**Correspondence to:**
H. Wang

**Email:**
whfcumt@126.com

**Dates:**
Received: 30 Jun. 2023
Revised: 9 Jan. 2024
Accepted: 9 Jan. 2024
Published: April 2024

**How to cite:**
Zhang, Z., Xu, Y., Wang, H., Shi, J., Niu, J., and Zhang, Z. 2024. Triboelectric characteristics and separation of magnesite and quartz. *Journal of the Southern African Institute of Mining and Metallurgy*, vol. 124, no. 4, pp. 193–200

**DOI ID:**
http://dx.doi.org/10.17159/2411-9717/2884/2024

## Abstract

**Tribo-electrostatic separation is a promising method for effectively utiliing low-grade magnesite resources by removing quartz and improving the grade of magnesite. To determine the charge-to-mass ratios of pure magnesite and quartz, a triboelectric measurement system was employed, and a laboratory tribo-electrostatic separation system was used to separate low-grade magnesite. The results showed that the maximum difference in charge-to-mass ratio between pure magnesite and quartz particles was observed after friction with polyvinyl chloride. The grade and recovery of magnesite increased with temperature and initially increased with increasing voltage, feed rate, and air flowrate before gradually decreasing. The optimal conditions resulted in a concentrate with 46.91% MgO content and 77.36% recovery, while the quartz content decreased from 7.02% to 1.95%. These experimental results demonstrate the effectiveness and potential of tribo-electrostatic separation in removing quartz and upgrading magnesite.**

## Keywords

**magnesite, tribo-electrostatic separation, tribo-charging characteristics, charge-to-mass ratio**

## Introduction

Magnesite is a crucial raw material in the production of magnesium metal, refractory materials, magnesium chemicals, and magnesium oxide (MgO), which have extensive applications in metallurgy, aerospace, and other industries (El-Sayed, 2018; Sun et al., 2021a; Sun et al., 2023; Wang et al., 2022). As a strategic mineral, magnesite plays a vital role in the economic development of most nations, including China, where it is abundant (Al-Mallahi et al., 2020; Han et al., 2020; Hu et al., 2020; Zhu et al., 2023). Unfortunately, the over-exploitation of high-grade magnesite resources has led to depletion of high-quality mines and the abandonment of numerous low-grade mines, causing both waste of magnesium resources and significant damage to the environment. This situation has become more pressing due to the increasing demand for magnesium ore (Shen et al., 2023; Sun et al., 2021b; Wang et al., 2022). Consequently, the development and utilization of low-grade magnesite resources is crucial, and it is imperative to employ advanced technology, equipment, and processing to fully utilize the available resources.

Flotation is currently considered the most effective way to separate magnesite and remove impurities (Brezáni et al., 2017; Sun et al., 2021c; Zhu et al., 2015). However, this method has strict requirements on particle size and is associated with high processing costs (Fan et al., 2021; Williams et al., 2022; Zhang et al., 2020; Zhang et al., 2023). Moreover, the wastewater and chemicals generated during the separation process lead to environmental pollution and resource waste, which is not in line with the government's green and low-carbon economic plan (Bentli et al., 2017; Wu et al., 2004). Additionally, abundant magnesite resources in the Xinjiang Uygur Autonomous Region of China cannot be utilized for flotation due to the scarcity of water (Wang et al., 2019a). In contrast, tribo-electrostatic separation technology is a dry beneficiation method that incurs low ecological costs, causes no pollution, and requires no water (Kianezhad and Raouf, 2020; Wang et al., 2017; Wang et al., 2018; Wang et al., 2019b). The resulting concentrate can be directly used for subsequent processing and has significant research and application potential in magnesite beneficiation.

Electrostatic separation is a solid sorting technique that relies on the variation in electrical properties between minerals (Dizdar et al., 2018). It encompasses a range of methods, such as dielectric separation, tribo-electrostatic separation, electrical classification, and high-gradient separation. Tribo-electrostatic separation is a type of electrostatic separation that exploits the difference in triboelectric charge between particles. The process generates charges of opposite polarity on the particles, which can be efficiently

separated by an electric field force. Tribo-electrostatic separation is a straightforward and cost-effective approach with enormous development potential and wide-ranging applications (Matsusaka et al., 2010; Mirkowska et al., 2014; Mirkowska et al., 2016). Bittner et al. (2014) described a triboelectric belt separator for beneficiation of fine minerals with an energy consumption of 1 kWh/t of materials processed.

This study investigated the triboelectric charging properties and sorting efficiency of magnesite by utilising a charge-to-mass ratio (*Q*/*m*) experimental system and tribo-electrostatic separation system. The impacts of materials and temperature on the triboelectric charging properties and of operating parameters on the sorting efficiency during tribo-electrostatic separation were analyzed. These findings provide an effective dry separation method for low-grade magnesite, which holds significant importance for promoting industrial applications of triboelectric separation. Tribo-electrostatic separation also has great potential in the preparation of ultra-pure coal, desiliconization of calcium carbide slag, decarburization of fly ash, and the beneficiation of calcium carbonate, limestone, and barite. In addition, it can be used in feldspar, iron ore, bauxite, potassium fertilizer, phosphate ore sorting, and enrichment of food and feed.

## Experimental

### *Charge-to-mass ratio test system*

In this study, the *Q*/*m* is utilized to describe the charge generated after friction between the friction medium and material particles. The *Q*/*m* is defined as the ratio of charge to the mass of the charged body (nC/g). The measurement system is illustrated in Figure 1. It primarily consists of a constant-temperature and -humidity chamber, stirrer, stirring rod made of various materials, stirring cup, Faraday cylinder, and an electrometer.

### *Tribo-electrostatic separation system*

The tribo-electrostatic separation system is illustrated in Figure 2. It consists of a Roots blower, gas storage tank, air heater, rotameter, screw feeder, bellows friction charger, high-voltage power supply, separation chamber, and an aggregator. The air-supply device, including the Roots blower and air storage tank, supplies the airflow for the entire system, which is heated to a predetermined temperature by the air heater. The material is transported to the pipeline by the screw feeder and delivered to the bellows friction charger under the influence of the airflow. The material particles are charged in the friction charger by continuous collisions between particles and between particles and the walls. The charged particles are then transferred to the separation chamber by the airflow. Under the effect of the electric force, the charged particles move to the separation chamber. The positively charged particles move to the side near the negative plate, while the negatively charged particles move to the side near the positive plate. Finally, the product is collected by the aggregator.

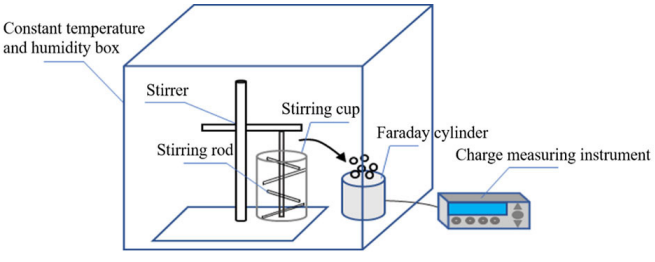


**Figure 1— Charge-to-mass ratio measurement system**

### *Materials characterization*

The magnesite sample utilized in this study was sourced from Liaoning province, China. X-ray diffraction (XRD) was used to analyze the mineral composition and determine the primary gangue minerals present. X-ray fluorescence (XRF) spectroscopy was utilized to determine the grade. Prior to the XRD and XRF analyses, the material was crushed to −74 μm. The results of the analyses are presented in Figure 3 and Table I. As per the XRF analysis, the MgO content was 45.36%, which indicates a low-grade magnesite. Based on the XRD results, the primary minerals present were magnesite and quartz, while the gangue contained a quartz content of 7.02%.

Scanning electron microscopy (SEM) and energy-dispersive spectra of the magnesite are presented in Figure 4. The SEM results indicate that magnesite and quartz were fully dissociated when the particle size was less than 74 μm. This dissociation provides a basis for the successful separation of magnesite and quartz using electrostatic separation.

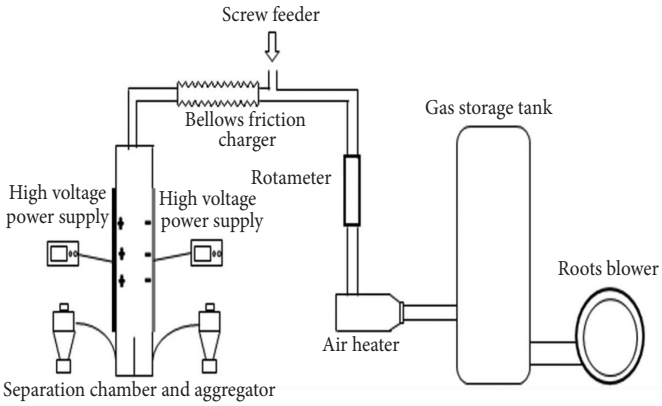


**Figure 2—Laboratory tribo-electrostatic separation system**

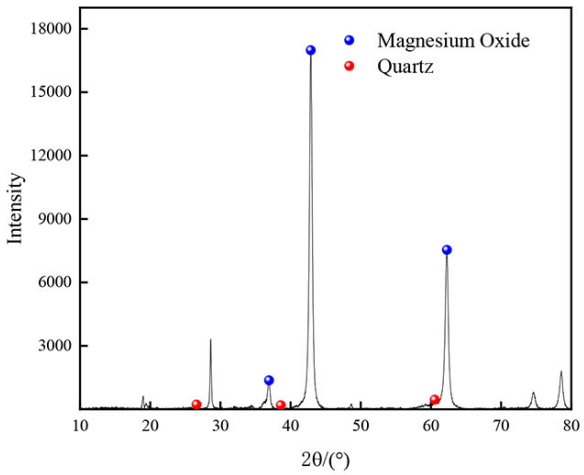


**Figure 3— X-ray diffraction spectrum of magnesite ore**

*Table I*

**X-ray fluorescence analysis results**

| Element | MgO | $SiO_2$ | CaO | $Fe_2O_3$ | $Al_2O_3$ | $CO_3$ |
|---|---|---|---|---|---|---|
| Content (%) | 45.36 | 7.02 | 0.54 | 0.51 | 0.52 | 46.05 |

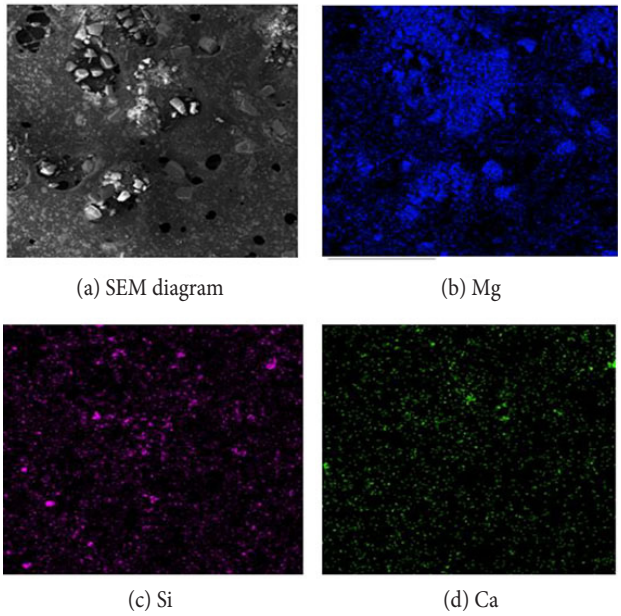


**Figure 4—(a) Scanning electron microscopy image of magnesite with particle size less than 74 µm. Energy-dispersive spectra of (b) Mg, (c) Si, and (d) Ca**

## Results and Discussion

### *Tribo-charging characteristics of magnesite*

Numerous theoretical and experimental studies have demonstrated that the triboelectric charging characteristics of particles play a crucial role in the tribo-electrostatic separation process (Dizdar et al., 2018; Wang et al., 2018; Wang et al., 2019a; Wang et al., 2019b). This study investigated the charge-transfer mechanism of magnesite and quartz during frictional charging at the microscopic level using atomic force microscopy. The results are presented in Figure 5, where Figure 5(a) illustrates that the surface potential of quartz was mostly green and relatively stable before charging, which enabled measurement of the surface potential after charging. From Figure 5(b), it can be observed that the surface potential of quartz turned blue after charging, with the blue area representing the charging area. The data in Figure 5(e) clearly show that the surface potential of quartz changed by −161 mV after charging. This confirms that charge transfer occurred on the surface of magnesite and quartz, where the surface of quartz was negatively charged due to the gain of electrons and the surface of magnesite was positively charged due to the loss of electrons. The surface potential of magnesite is lower than that of quartz, and the surfaces of the two minerals carried opposite charges. This phenomenon is the basis for the frictional electrostatic sorting of magnesite and quartz.

The aim of the experiment was to investigate the effects of different tribocharging materials; namely, polyvinyl choride (PVC), polypropylene (PP), polyethylene (PE), and copper (Cu), on the surface potential and topography of quartz before and after charging. Figure 6 presents the results obtained. Before charging, the quartz surface potential diagram was green, indicating a stable potential. After friction and charging with the four materials, charged areas appear on the diagram. Specifically, after PP and PE particles were charged by friction with quartz, blue areas appeared on the surface potential diagram, indicating that the quartz surface gained electron charge, while the PP and PE particles lost electron charge. The surface potential of quartz decreased, and those of PP and PE particles were lower than that of quartz. After friction and charging with PVC and copper particles, red areas appeared on the quartz surface potential diagram, indicating that the surface of quartz lost electron charge, and the surfaces of PVC and copper particles gained electron charge. The surface potential of quartz rose, and the surface potentials of PVC and copper particles were higher than that of quartz. Comparison with the colour scale on the right confirmed the occurrence of charge transfer between the tribocharging materials and quartz surface.

The study also examined the *Q/m* variation of the particle population on a macroscopic scale. This involved investigating changes in the *Q/m* between magnesite and various friction materials, as well as the impact of temperature. The results provide important insights into selecting appropriate friction materials and temperatures during sorting tests. The study tested the effect of different temperatures (20–60°C) using PVC, PP, PE, and Cu as tribocharging materials.

In Figure 7, it is observed that magnesite particles became positively charged by losing electrons on their surface when triboelectrically charged with the four different friction materials. The surface potential of magnesite was lower than those of the four friction materials. At a temperature of 40°C, the *Q/m* of magnesite after friction with PVC, PP, PE, and Cu were 3.74 nC/g, 2.47 nC/g, 2.19 nC/g, and 1.23 nC/g, respectively. The *Q/m* of magnesite to PVC, PP, and PE exceeded 2.0 nC/g, whereas that to Cu was relatively low. These results suggest that PVC, PP, and PE are more suitable friction materials for magnesite separation, and the optimal temperature for the tribo-charging of magnesite is around 40°C.

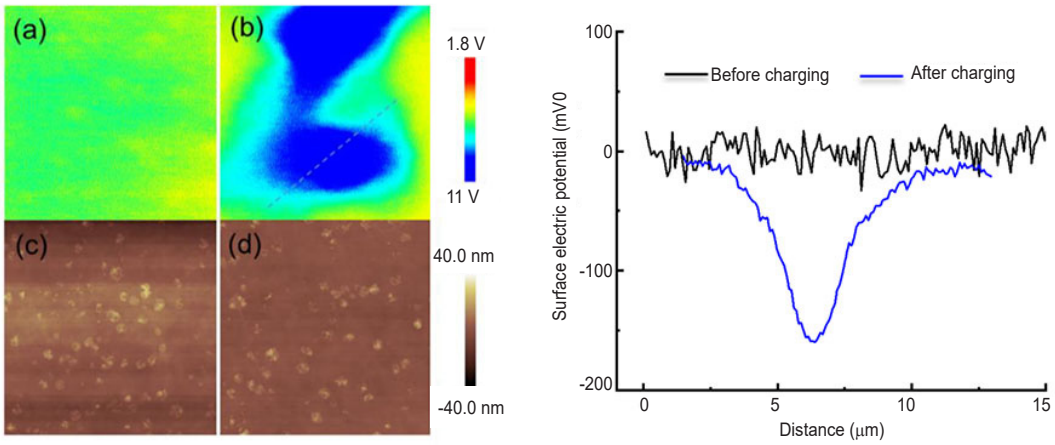


**Figure 5—Surface electric potentials of quartz and magnesite before and after charging**

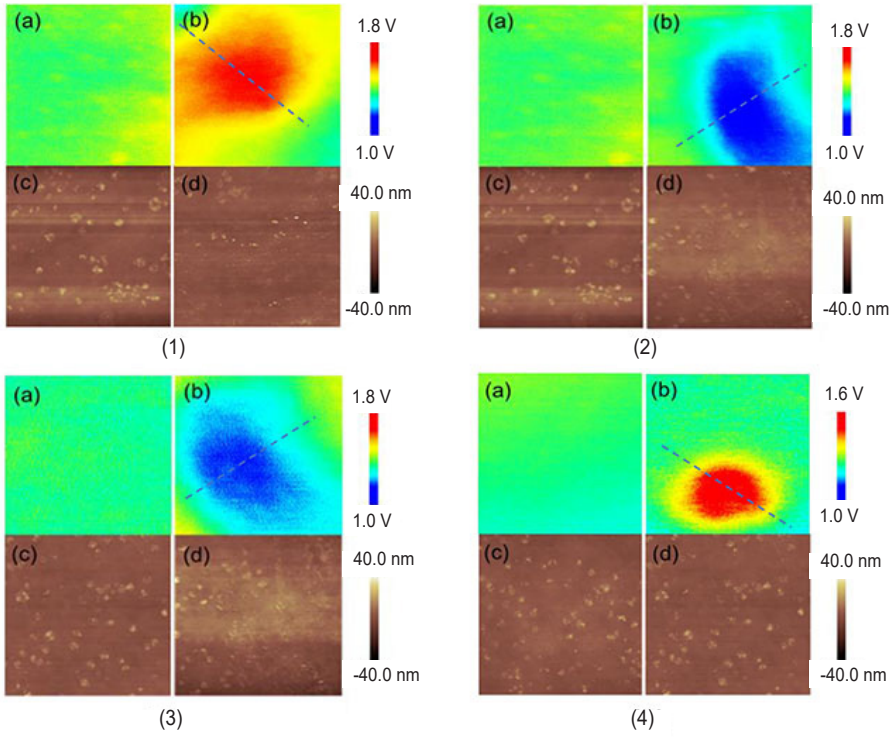


**Figure 6—Surface potentials and morphologies of quartz and four types of material particles before and after charging: (1) polyvinyl chloride, (2) polypropylene, (3) polyethylene, and (4) copper**

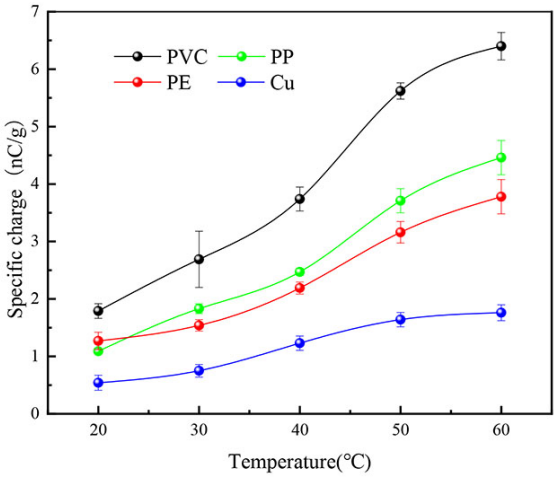


**Figure 7—Variation of charge-to-mass ratio of friction between magnesite and different materials at different temperatures**

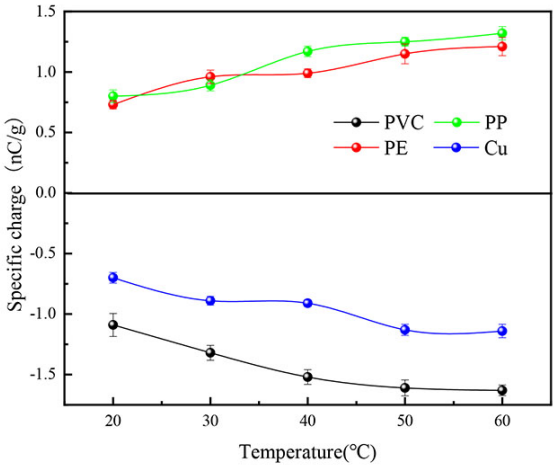


**Figure 8—Variation of charge-to-mass ratio of friction between quartz and different materials at different temperatures**

The *Q*/*m* is affected by temperature, with the ratio gradually increasing as the temperature increases. However, the rate of change of the charge-to-mass ratio initially increased with temperature and then gradually decreased. It is important to note that the number of free electrons on the surfaces of both magnesite particles and the frictional materials increased with temperature. As the temperature increased, the amount of charge transfer between magnesite particles and frictional material increased due to enhanced frictional charging during their collision, leading to an increase in *Q*/*m*.

Figure 8 shows that when quartz particles were triboelectrically charged with PVC and Cu, the surface potential became negative due to the release of electrons, and the surface potential of quartz was higher than those of PVC and Cu. In contrast, when quartz particles were triboelectrically charged with PP and PE, their surface became positively charged due to transfer of electrons, and its surface potential became lower than those of PP and PE. At a temperature of 40°C, *Q*/*m* of quartz with PVC, PP, PE, and Cu after friction were −1.52 nC/g, 1.17 nC/g, 0.99 nC/g, and −0.91 nC/g, respectively. The change in *Q*/*m* with temperature after friction charging between quartz particles and different friction materials is similar to that observed for magnesite. As the temperature increased, *Q*/*m* continued to increase, and the rate of change of *Q*/*m* initially increased, followed by a gradual decrease.

The variation of *Q*/*m* of magnesite and quartz particles after friction with different materials is similar. However, *Q*/*m* of magnesite particles after friction was larger than that of quartz

particles. At 40ºC, *Q/m* differences between magnesite and quartz with PVC, PP, PE, and Cu were 5.26 nC/g, 1.3 nC/g, 1.2 nC/g, and 3.2 nC/g, respectively. The order of the difference is PVC > PP > PE > Cu. Although *Q/m* of magnesite and quartz particles rubbed with PP and PE differed slightly, they had the same charge-to-electrode polarity after rubbing and were challenging to effectively separate under an electric field. Magnesite and quartz particles had opposite polarity to charged electrodes after friction with PVC and Cu materials, and they could move to opposite sides of the polar plate under the electric field, satisfying the requirements for friction materials. However, *Q/m* difference between magnesite and quartz particles and PVC after friction was significantly larger than that with Cu. Under the same electric field intensity, PVC is expected to have better separation efficiency than Cu. Despite the relatively small *Q/m* difference after Cu friction, its charge-to-electrode polarity meets the requirements. Additionally, Cu is stronger and more durable than PVC. Thus, Cu appears to be a promising choice for the frictional material.

### *Influence of temperature on tribo-electrostatic separation*

We examined the impact of temperature on the tribo-electrostatic separation process by analysing the tribo-charging characteristics. The charging effect in a triboelectric charger is the key factor that influences material separation in this separation system. We thus investigated the effect of temperature on the separation of magnesite particles.

The contents of magnesia and quartz in magnesite products are used to grade them; thus, the contents of magnesia and quartz in the concentrate and recovery of magnesia were chosen as the primary evaluation criteria for the effect of magnesite electrification. Figure 9 displays that temperature has an impact on the contents of magnesium oxide and quartz in the positive and negative electrodes, as well as the recovery of magnesium oxide. Figure 9(a) reveals that as the temperature increased, the MgO content in the concentrate also increased. The growth rate initially rose with increasing temperature and then gradually declined. The temperature range of 40–50°C showed the fastest growth and the content tended to stabilize above this range. The highest MgO content of 46.56% was observed at 60°C. Conversely, the content of quartz in the concentrate continuously decreased as the temperature rose, with the minimum content of quartz being 2.33% at 60°C. The change in quartz content was opposite to the change in MgO content.

Figure 9(b) reveals that recovery of MgO increased with temperature, reaching a maximum of 66.2%. This finding, in combination with analysis of the temperature-dependent *Q/m*, indicates that magnesite and quartz have relatively few free electrons on their surface at room temperature. Additionally, their surface charge barely changes after particle collision, resulting in little change to the grade and recovery of magnesite. However, an increase in temperature leads to an increase in the number of free electrons on the surface of magnesite and quartz, resulting in stronger electric field forces during the sorting process after particle collision. This enhanced sorting effect ultimately leads to an increase in the grade and recovery of magnesite in the concentrate. The grade and recovery of magnesite stabilized at 60°C.

### *Tribo-electrostatic separation of magnesite*

### *Influence of sorting voltage on tribo-electrostatic separation*

The separation of different electrified minerals is achieved by the change in particle movement trajectory due to their differences in particle charge and charge properties, which moves them to the two polar plates under the influence of the electric field force. The electric field force acting on the charged particles during their movement is determined by the sorting voltage, which is the distance between the two plates. In this study, we investigated the separation of magnesite under different separation voltages. Figure 10 illustrates that the MgO content in the concentrate initially increased with an increase in separation voltage, followed by a decrease, while the opposite effect was shown by quartz. The highest MgO content of 46.57% and the lowest quartz content of 2.33% were obtained at a sorting voltage of 15 kV. Additionally, Figure 10 shows that the recovery of MgO in the concentrate increased with the increase in separation voltage, up to 15 kV; however, when the voltage exceeded 15 kV, the recovery started to decrease. The maximum recovery of MgO of 72.88% was observed at 15 kV.

In summary, the sorting voltage plays a crucial role in the separation of charged particles in the electric field. When the sorting voltage was less than 15 kV, the electric field force on the charged particles increases, resulting in longer lateral movement distance of particles within the electric field. This effectively separated the charged particles and improved the sorting effect. However, when the sorting voltage exceeded 15 kV, the particles with low or high charges polarized after contacting two sides of the electrode plates, leading to mixing of the charged particles and reduction in the sorting effect. Therefore, optimal sorting was achieved at a sorting voltage of 15 kV.

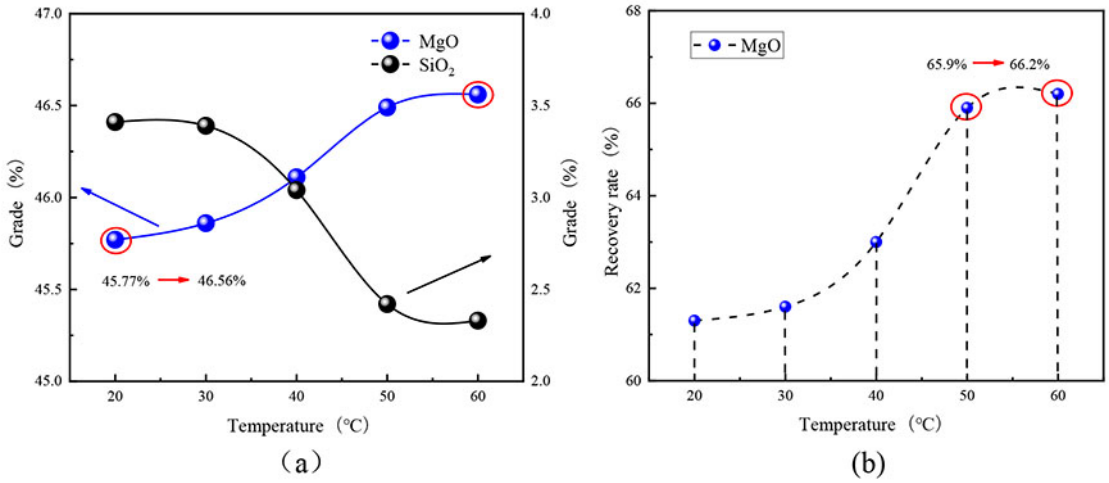


**Figure 9—Influence of temperature on (a) grades of magnesite and quartz and (b) recovery of magnesite**

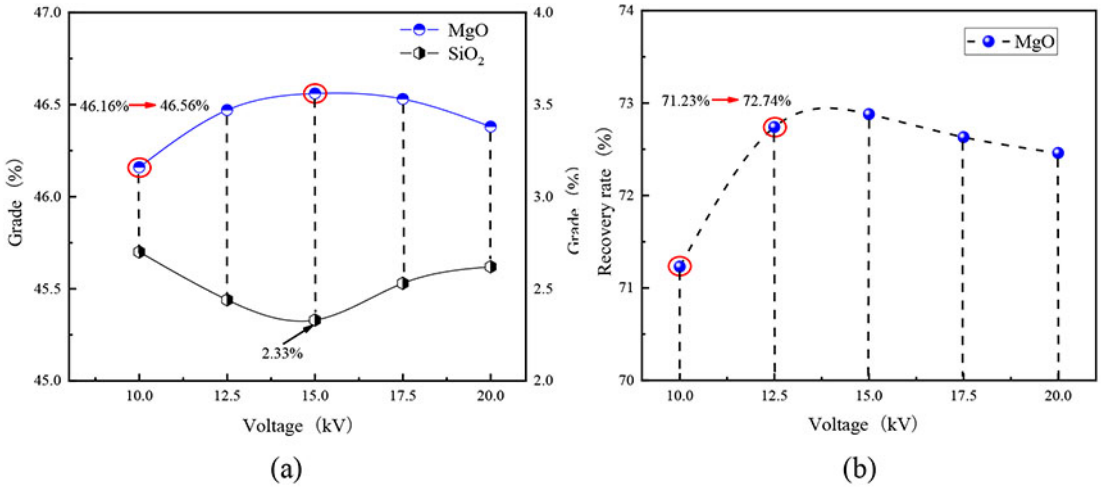


**Figure 10—Influence of sorting voltage on (a) grades of magnesium oxide and quartz and (b) recovery of magnesium oxide**

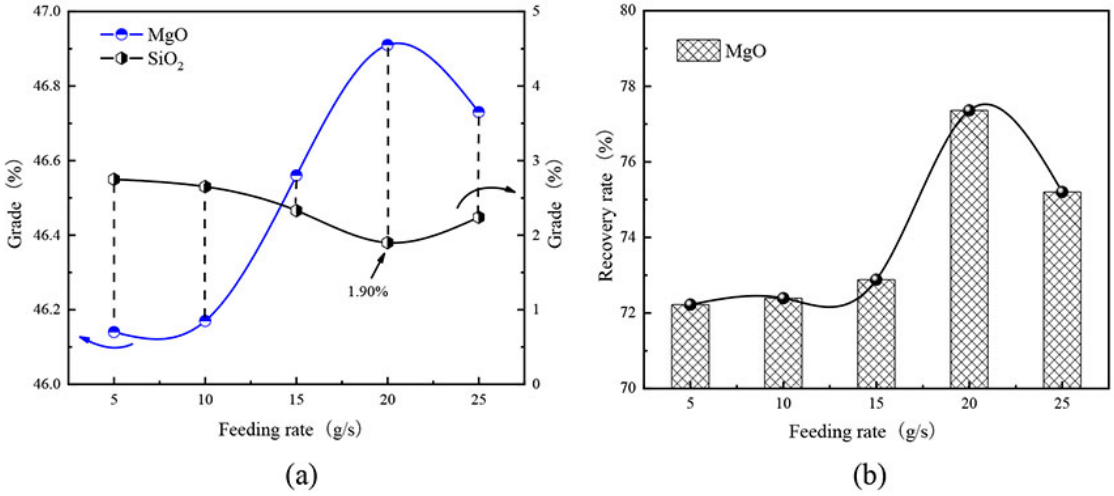


**Figure 11—Effect of feed rate on (a) grades of magnesium oxide and quartz and (b) recovery of magnesium oxide**

### *Influence of feed rate on tribo-electrostatic separation*

The collision frequency in the friction charger, which determines the quality of sorting, is affected by the feed rate at certain airflow speeds. As depicted in Figure 11, when the feed rate was below 20 g/s, the MgO content in the concentrate continuously increased, while the quartz content decreased. Conversely, when the feed rate was above 20 g/s, the quartz content in the concentrate started to increase, while the MgO content decreased. The highest MgO content in the concentrate was 46.91% and the lowest quartz content was 1.9%. Figure 11 reveals that, when the feed rate was below 20 g/s, the recovery of MgO in the concentrate increased with the increase in feed rate, while the change in quartz content initially increased with the feed rate and then gradually decreased. When the feed rate was above 20 g/s, the recovery of MgO in the concentrate decreased with the increase in feed rate. The maximum recovery of MgO was 77.36%.

The feed rate plays a crucial role in determining the sorting effect by affecting the collision frequency in the friction charger, which is subject to a certain airflow speed. At low feed rates, the number of particles in the friction charger was small, resulting in low turbulence intensity and low frequency of particle-to-particle or particle-to-friction-charger sidewall collisions. This resulted in low tribo-charging of the particle surface, which reduced the effect of electric field force in the separation chamber, causing ineffective separation and low concentrate grade and recovery. As the feed rate increased, the number of particles in the friction charger increased, and the gas flow rate fluctuated more, resulting in higher turbulence intensity and collision frequency. The resulting increase in particle charge and the effect of electric field force enhanced the separation process, leading to a higher concentrate grade and recovery. However, when the feed rate was too high, the collision frequency between particles and sidewalls decreased, leading to material accumulation, lower particle charge, weaker electric field force, and a decrease in the concentrate grade and recovery. Therefore, the optimal sorting effect occurred at a feed rate of 20 g/s.

### *Influence of airflow speed on tribo-electrostatic separation*

The airflow speed plays a crucial role in determining the collision frequency, collision intensity, and movement time of charged particles in the sorting process, thereby impacting the sorting effect. Figure 12 illustrates that, for airflow velocities below 60 $m^3/h$, the MgO content in the concentrate continuously increased, while the quartz content decreased. Conversely, when the airflow velocity was greater than 60 $m^3/h$, the MgO content decreased and the quartz content increased. The concentrate displayed the highest MgO content (46.91%) and lowest quartz content (1.9%). Moreover, Figure 12 shows that, when the airflow velocity was less than 60 $m^3/h$, the recovery of MgO in the concentrate increased with

feed rate. Additionally, the MgO content increased with increasing airflow velocities. However, the recovery decreased with increasing feed rate. The maximum recovery of MgO was 77.36%.

The magnitude of the airflow velocity had a significant impact on the quality of sorting during electrostatic separation of magnesite, because it affected both the collision frequency and intensity of particles in the friction charger and the movement time of charged particles in the sorting chamber under the influence of the electric field. At low airflow velocities, the collision frequency and electrical charge of particles were low, resulting in ineffective separation due to the weak effect of the electric field force, resulting in low recovery of MgO. However, increasing the airflow velocity led to an increase in the movement speed and disorder of particles, as well as their electrical charge and the effectiveness of the electric field force, thereby enhancing the recovery of MgO. Nonetheless, if the airflow velocity exceeded a certain value, the movement time of charged particles in the sorting chamber reduced, thereby reducing the recovery of MgO. Consequently, it is essential to maintain a controlled airflow velocity to ensure optimal sorting of magnesite during electrostatic separation.

## Conclusions

Based on the current results, several conclusions can be made:

(1) When PP and PE were used as the frictional materials, magnesite and quartz particles had the same charge polarity, which made it challenging to effectively separate them. However, when friction occurred between the particles and PVC or Cu, the magnesite and quartz particles acquired an opposite charge polarity to the electrode, which enabled them to move towards opposite sides of the electrode plate and achieve high-quality separation. Magnesite and quartz particles exhibited significantly different $Q/m$ after friction with PVC, resulting in excellent separation efficiency.

(2) Increasing the temperature resulted in an increase in the number of free electrons on the surface of magnesite particles and friction material. This led to higher charge transfer, frictional charging, and $Q/m$ during frictional collision between the particles and friction material. The change rate of $Q/m$ initially increased with temperature and then gradually decreased.

(3) Raising the sorting voltage increased the electric field force on the charged particles and lateral movement distance of particles in the electric field. This increase in force effectively separated the charged particles and improved the sorting effect. However, if the sorting voltage was too high, particles with a lower or higher electric charge became polarized upon contact with the plates on both sides. As a result, charged particles entered the positive and negative products without separation, leading to a reduced sorting effect.

(4) The grade and recovery of magnesite depend on the amount of charge in the friction charger and the movement time under the influence of the electric field in the sorting chamber. When the collision frequency of particles was low, the amount of charge and effect of electric field force were also low, and particles could not be effectively separated. In contrast, increasing the particle movement speed led to an increase in particle charge and strengthening by the electric field force, which enhanced the charging effect and recovery of magnesite. Therefore, to ensure effective separation of magnesite, operating parameters such as feed velocity and airflow velocity should be controlled.

## Recommendations

Tribo-electrostatic separation offers various advantages, such as minimal maintenance, a completely dry process without the need for water and chemicals, a high specific feed rate, ease of operation, and environmental friendliness. The energy consumption is low, estimated to be no more than 4 kWh/t of processed materials according to the laboratory test unit.

In the next phase, we will investigate the micro-friction charging mechanism of magnesite and optimize the structure and materials of the bellows friction charger. Our aim is to enhance the separation effect by strengthening the friction charging process. Simultaneously, we are developing a new type of separation machine and accompanying devices to augment processing capacity while ensuring effective separation. The optimization efforts will progress from semi-industrialization to full industrial applications.

## Acknowledgements

The authors acknowledge financial support by the Jiangsu Provincial Key R&D Plan (Social Development) Project (BE2022717) and the National Nature Science Foundation of China (51674257).

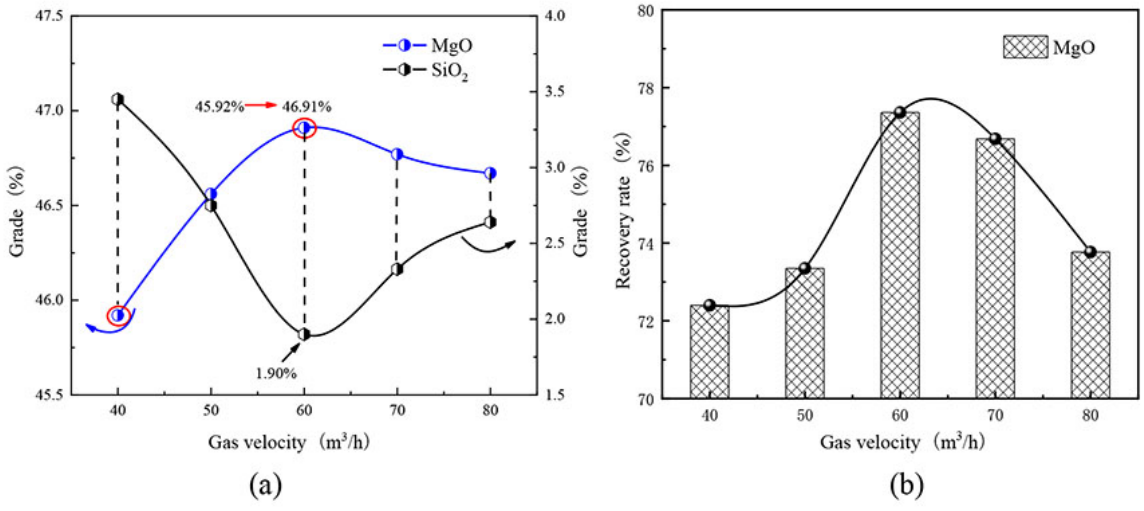


**Figure 12—Effect of gas flow rate on (a) grades of magnesia and quartz and (b) recovery of magnesium oxide**

## References


Al-Mallahi, J., Surmeli, R. O., and Calli, B. 2020. Recovery of phosphorus from liquid digestate using waste magnesite dust. *Journal of Cleaner Production*, vol. 272, p. 122616.

Bentli, I., Erdogan, N., Elmas, N., and Kaya, M. 2017. Magnesite concentration technology and caustic-calcined product from Turkish magnesite middlings by calcination and magnetic separation. *Separation Science*, vol. 52, no. 6, pp. 1129–1142.

Bittner, J.D., Hrach, F.J., Gasiorowski, S.A., and Guicherd, H. 2014. Triboelectric belt separator for beneficiation of fine minerals. *Procedia Engineering*, vol. 83, pp. 122–129.

Brezáni, I., Škvarla, J., and Sisol, M. 2017. Reverse froth flotation of magnesite ore by using (12-4-12) cationic gemini surfactant. *Minerals Engineering*, vol. 110, pp. 65–68.

Dizdar, T., Kocausta, G., Gulcan, E., and Gulsoy, O. 2018. A new method to produce high voltage static electric load for electrostatic separation: triboelectric charging. *Powder Technology*, vol. 327, pp. 89–95.

El-Sayed, M.A. 2018. An investigation of the behaviour of double oxide film defects in aluminium-magnesium cast alloys. *Journal of the Southern African Institute of Mining and Metallurgy*, vol. 118, no. 11, pp. 1225–1231.

Fan, X. and Zhou, C. 2021. Estimation of bed expansion and separation density of gas-solid separation fluidized beds using a micron-sized-particle dense medium. *Separations*, vol. 8, no. 12, pp. 242.

Han, C., Zhang, H., Tan, R., Shen, Y., and Liu, W. 2020. Effects of monohydric alcohols of varying chain lengths and isomeric structures on magnesite and dolomite flotation by dodecylamine. *Powder Technology*, vol. 374, pp. 233–240.

Hu, Y.C. 2020. Constructing grey prediction models using grey relational analysis and neural networks for magnesium material demand forecasting. *Applied Soft Computing*, vol. 93, p. 106398.

Kianezhad, M. and Raouf, A.H. 2020. Improvement of tensile and impact properties of 5083 aluminium weldments using fillers containing nano-$Al_2O_3$ and post-weld friction stir processing. *Journal of the Southern African Institute of Mining and Metallurgy*, vol. 120, no. 4, pp. 277–286.

Matsusaka, S., Maruyama, H., Matsuyama, T., and Ghadiri, M. 2010. Triboelectric charging of powders: A review. *Chemical Engineering Science*, vol. 65, no. 22, pp. 5781–5807.

Mirkowska, M., Kratzer, M., Teichert, C., and Flachberger, H. 2014. Atomic force microscopy as a tool to explore triboelectrostatic phenomena in mineral processing. *Chemie Ingenieur Technik*, vol. 86, no. 6, pp. 857–864.

Mirkowska, M., Kratzer, M., Teichert, C., and Flachberger, H. 2016. Principal factors of contact charging of minerals for a successful triboelectrostatic separation process – a review. *BHM Berg und Huttenmannische Monatshefte*, vol. 161, no. 8, pp. 359–382.

Shen, X., Huang, Y., Shao, H., Liu, Y., Gu, H., and Zhai, Y. 2023. Improvement of utilization efficiency of magnesite by $(NH_4)_2SO_4$ roasting–water leaching process. *Transactions of Nonferrous Metals Society of China*, vol. 33, no. 2, pp. 576–583.

Sun, W., Dai, S., Liu, W., Li, P., and Yu, X. 2021a. Effect of Ca(II) on anionic/cationic flotation of magnesite ore. *Minerals Engineering*, vol. 163, p. 106778.

Sun, H., Yin, W., Yang, B., Chen, K., and Sheng, Q. 2021b. Efficiently separating magnesite from quartz using n-hexadecyltrimethylammonium chloride as a collector via reverse flotation. *Minerals Engineering*, vol. 166, p. 106899.

Sun, H., Yang, B., Zhu, Z., Yin, W., Sheng, Q., Hou, Y., and Yao, J. 2021c. New insights into selective-depression mechanism of novel depressant EDTMPS on magnesite and quartz surfaces: Adsorption mechanism, DFT calculations, and adsorption model. *Minerals Engineering*, vol. 160, p. 106660.

Sun, Z., Zhao, Y., Yan, G., Yuan, H., Zhang, M., and Zhang, B. 2023. A novel method for low-rank coal drying using steam transient flash evaporation. *Fuel*, vol. 354, p. 129238.

Wang, H., Zhang, G., Hao, J., He, Y., Zhang, T., and Yang, X. 2017. Morphology, mineralogy and separation characteristics of nonmetallic fractions from waste printed circuit boards. *Journal of Cleaner Production*, vol. 170, pp. 1501–1507.

Wang, H., Fotovat, F., Bi, X.T., and Grace, J.R. 2018. Tribo-charging of binary mixtures composed of coarse and fine particles in gas–solid pipe flow. *Particuology*, vol. 43, pp. 101–109.

Wang, Z., Cao, Y., Xing, Z., Wang, J., and Li, G. 2019a. Experimental study on fragmentation of magnesite ores by pulsed high-voltage discharge. *Transactions of China Electrotechnical Society*, vol. 34, no. 4, pp. 863–870.

Wang, H., Bai, X., Peng, Z., Zhao, X., and He, Y. 2019b. Enrichment effect of coal and quartz particles in gas-solid fluidized bed with applied electrical field. *Powder Technology*, vol. 354, pp. 743–749.

Wang, Y., He, G., Abudukade, D., Li, K., Guo, T., Li, S., Xiao, Z., Wang, J., and Nie, S. 2022. Selective inhibition of sodium tripolyphosphate on calcite in the process of magnesite flotation. *Journal of Molecular Liquids*, vol. 345, p. 117412.

Williams, O.S.A., Daley, P., Perkins, J., Martinez-Mendoza, K.L., Guerrero-Perrez, J., Mazabuel, L.M.S., Saavedra, E.A.G., Trujillo, M., Barraza-Burgos, J., Baragas, M., Romero, M.H., and Lester, E.H. 2022. Upgrading of low-grade Colombian coals via low-cost and sustainable calcium nitrate dense media separation. *ACS Omega*, vol. 7, no. 4, pp. 3348–3358.

Wu, C., Zhou, P., Duan, X., and Dai, H. 2004. Study on application of dry electrostatic separation in chemical mine. *Environmental Protection of Chemical Industry*, vol. 1. pp. 9–12.

Zhang, Z., Yan, G., Zhu G., Zhao, P., Ma, Z., and Zhang, B. 2020. Using microwave pretreatment to improve the high-gradient magnetic-separation desulfurization of pulverized coal before combustion. *Fuel*, vol. 274, p. 117826.

Zhang, Z., Wei, X., Yan, G., Guo, J., Zhao, P., Yang, F., Zhao, H., and Zhang, B. 2023. Formation of pyrite in the process of fine coal desulfurization by microwave enhanced magnetic separation. *International Journal of Coal Preparation and Utilization*, vol. 43, no. 3, pp. 484–501.

Zhu, Y., Yan, X., Pan, K., and Li, Y. 2015. Research on flotation purification of low grade magnesite of Liaoning province. *China Mining Magazine*, vol. 24, no. 5, pp. 118–120.

Zhu, H., Shao, S., Guo, M., Zhang S., and Zhang, Y. 2023. Engineering properties and sustainability evaluation of crushed low grade magnesite mortars. *Journal of Cleaner Production*, vol. 425, p. 138979. ◆